

## Conservative indentation flow throughout thin (011) InP foils

L. LARGEAU, G. PATRIARCHE

*Laboratoire de Photonique et de Nanostructures, UPR 20 CNRS, Route de Nozay, 91460 Marcoussis, France*

E. LE BOURHIS

*Université de Poitiers, Laboratoire de Métallurgie Physique, UMR 6630 CNRS, SP2MI-Téléport 2-Bd Marie et Pierre Curie, B.P. 30179, 86962 Futuroscope-Chasseneuil Cedex, France*

J. P. RIVIERE

*Laboratoire de Physique des Solides et de Cristallogénèse, UMR 8635 CNRS, 1 Pl. A. Briand, 92195 Meudon Cedex, France*

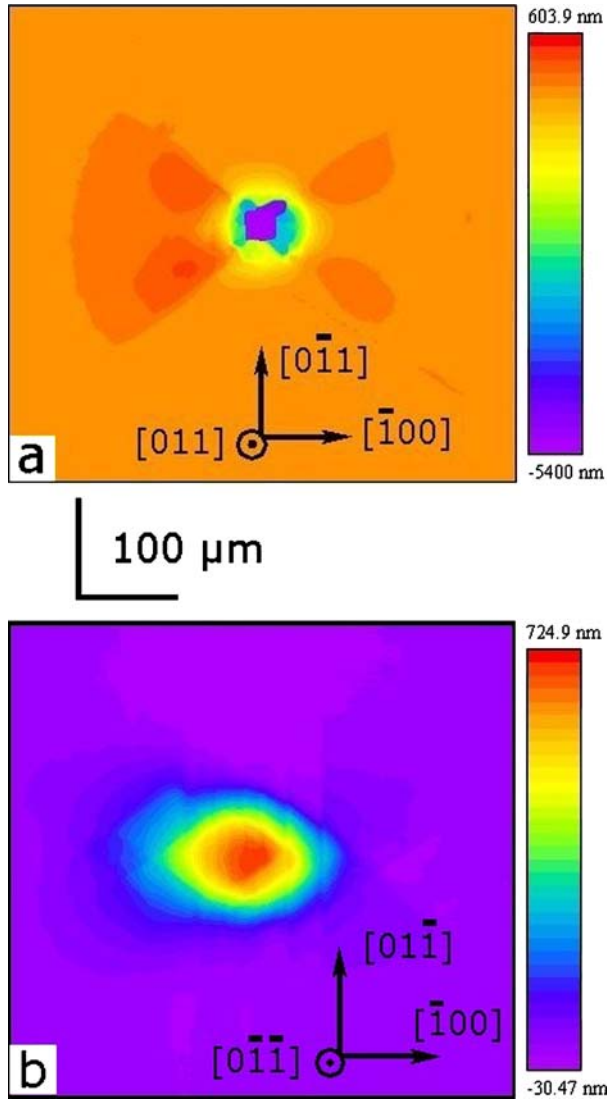
Development of III–V semiconductor heterostructures for optoelectronic applications has been limited, as plastic relaxation deleteriously affects the performance of the devices [1]. As the sizes of the structures decrease progressively, the plasticity of thin films has to be taken into account especially when considering temperatures around 400–500 °C necessary for the devices fabrication. Indentation tools allow to test small volumes (for a review refer to [1]), unfortunately nanoindentation at elevated temperature is very difficult to be performed [2] and most studies were reported at intermediate temperatures [3]. Here, we performed microindentation tests at 400 °C. Furthermore, contact mechanics was developed for semi-infinite isotropic half space [4]. It has been shown that deviations to the ‘cavity’ model happen when the size of the plastic zone becomes of the order of one dimension of the object [5, 6]. In [6], we showed that when thin foils of (011) InP were indented under increasing loads, material flow in normal {111} slip planes throughout the sample is detected while pile-ups progressively vanished at the indented surface. Here, we report an optical interferential study on indented thin foils of (011) InP, which permits a better understanding of the plastic flow events (pile-up and back side deformation) and demonstrates plastic flow conservation.

We used a Czochalski grown single crystal of (011) InP, which was not intentionally doped ( $n \sim 10^{16} \text{ cm}^{-3}$  Hall effect measurement). One of the faces was epitaxially, the other one was mechanically and chemically polished using a 1% bromine-methanol solution in order to obtain a 250  $\mu\text{m}$  thick sample with smooth surfaces. The thinned sample was deformed by a Vickers diamond pyramid at 400 °C in air atmosphere using five different loads ranging from 0.4 to 2.9 N. For each load the indentation test was repeated twice. The sample was set on a home-designed holder in which a 1.3 mm-wide trench was machined so that the bottom face of the sample underneath the indent site was not in contact with the holder. The load was applied for 60 s on the sample before the indenter was raised. One side of the indentation was aligned along the  $[0\bar{1}1]$  direction, the other one being aligned along the  $[100]$  orthogonal direction. We used a white-light interferometer (Micromap 570 ATOS, Pfungstadt Germany) operating at

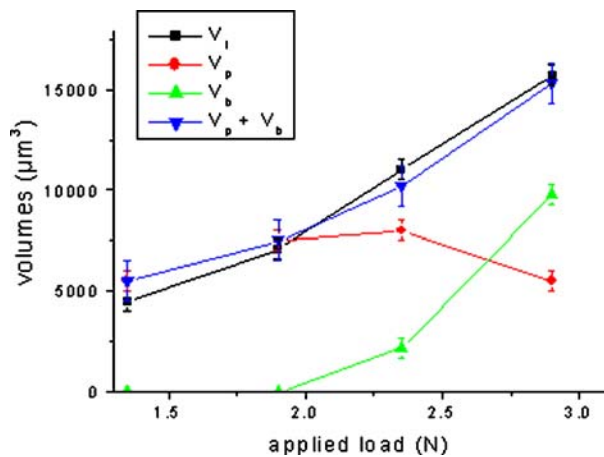
580 nm to obtain quantitative images of the surface topography of the indentation sites and of the opposite bottom surface.

Fig. 1 shows the surface topography of the indented side (Fig. 1a) and of the back side (Fig. 1b) obtained under the highest load used for this study (2.9 N). These topographical images can be usefully compared to observations made by optical microscopy and in the cathodoluminescent mode of the scanning electron microscope (Figs 2 and 3 in [3], respectively). Interferometry provides 2-dimensional (2D) topography of the plastically deformed zones and allows precise determining of the deformed volumes as discussed below.

On the topographic images obtained at the indented surface, we can observe the mark of the indentation that corresponds to levels below the original surface while pile-ups observed around the indent site correspond to levels above the original surface. As discussed below, under large loads pile-ups progressively vanish, however 2D optical interferometry allows detection of them even under the highest loads used here (2.9 N). In order to image the pile-ups, the resolution and the scale have been chosen accordingly. As a result, the indentation center is not properly resolved in the Fig. 1a. In fact the indentation center was detected at  $-11.5 \mu\text{m}$  below the original surface. This saturated scale permits enhancement of the contrast because of slight differences in height and detection under a 2.9 N load of four different pile-ups in a twofold symmetry. Along both  $\langle 100 \rangle$  directions, two pile-ups form a V-shaped zone with an angular aperture of about  $70^\circ$ . Interestingly, only one V-shaped zone (along  $[100]$ ) was observed on GaAs (011) surfaces indented at elevated temperature [7]. Pile-ups reveal reverse flow of matter in {111} planes inclined to the indented surface. At the  $[100]$  side they correspond to glide in  $(\bar{1}11)_{\text{B}}$  planes while at the  $[\bar{1}00]$  side they correspond to gliding in  $(111)_{\text{A}}$  planes. Hence, the anisotropy observed in GaAs may be attributed to the stronger polar character of GaAs as compared to InP. In fact, the difference in mobility between  $\alpha$  and  $\beta$  dislocations is more important in GaAs than in InP [8]. It should be noted that a slight anisotropy is detected in InP, as pile-ups at the  $[\bar{1}00]$  side are less pronounced than at the  $[100]$  side.



**Figure 1** White-light interferometer topographic images of a specimen deformed at 400 °C under 2.9 N. (a) Indented surface showing the indentation mark and pile-ups around the indent site. Note the twofold symmetry. (b) Back surface showing a diamond-shaped deformed area delimited by the emergence of {111} planes normal to the surface. In Fig. 1a, we fixed the lowest level at  $-5.4 \mu\text{m}$  so that the indentation center level is arbitrary (it is  $-11.5 \mu\text{m}$  below the original surface).



**Figure 2** Vickers mark, pile-ups and back-side deformed volumes ( $V_i$ ,  $V_p$ ,  $V_b$  respectively) as a function of the applied load.  $V_p + V_b$  is found to be equal to  $V_i$  within the uncertainty.

Observation of the back side of the sample showed a twofold symmetric plastically deformed zone. The plastic deformation is detected in an area that is diamond-shaped with sides parallel to the  $\langle 211 \rangle$  directions. These directions correspond to the emergence of  $\{111\}$  planes normal to the  $(0\bar{1}\bar{1})$  back surface. As discussed in more detail below, such deformation can be described by a punching mechanism on the basis of the development of dislocations loops with Burgers vector parallel to the  $[0\bar{1}\bar{1}]$  direction.

In the following we used 2D profilometry data to determine the plastically deformed volumes at the indented side and at the back side. A routine was developed to collect the height matrix  $h(x, y)$  defined at the sample positions  $(x, y)$  and to sum all elementary volumes. Thus, we obtained the volume of the pile-ups  $V_p$  that corresponds to the reverse flow of matter at the indented surface and the plastically deformed volume at the back side  $V_b$  that was punched throughout the sample.

$$V_p = \sum h_p(x, y) \delta x \delta y \quad (1)$$

$$V_b = \sum h_b(x, y) \delta x \delta y \quad (2)$$

where  $\delta x \delta y$  is the elementary specimen area (corresponding to one pixel in the image). Because of the large depth of the indentation marks, it is not possible to use the same method to determine precisely the volume of the marks. Alternatively, we measured the average diagonal size  $D$  by optical microscopy and the volume of the mark  $V_i$  is

$$V_i = 1/6 D^2 h_r \quad (3)$$

where  $h_r$  is the residual depth of the Vickers mark. In the following, we neglected the elastic recovery of the Vickers mark [2, 9] and took for  $h_r$  the contact depth value  $h_c$  that is geometrically determined as

$$h_c = D/7 \quad (4)$$

Fig. 3 plots the three different volumes ( $V_i$ ,  $V_p$ ,  $V_b$ ) as a function of the applied load. When load is increased, 'material transfer' to the back side, which can be defined as  $V_p/V_i$ , increases progressively. It can be concluded that plastic flow throughout the specimens becomes dominant. Furthermore, as shown in Fig. 3, the volume of the indentation mark is determined to be almost equal to the sum of the pile-ups volume and the back-side deformed volume showing that indentation plastic flow is conservative.

$$V_i = V_b + V_p \quad (5)$$

Interestingly, this experimental result has no dependence on the applied load. Hence Equation 5 is valid whether the sample can be considered as infinite ( $V_b \sim 0$ ) or as finite ( $V_b > 0$ ). Equation 5 implies that when the punching mechanism occurs ( $V_b > 0$ ), the pile-ups first diminish and finally disappear and that both events are related. Following the plastic-flow model proposed

in [3, 4], dislocations with Burgers vector parallel to the loading direction ( $b = a/2[0\bar{1}\bar{1}]$ ) do not reach the back surface under the lowest loads used here. Decomposition and deviation of these dislocations into dislocations gliding in  $\{111\}$  inclined slip planes lead to the pile-up formations observed around the indent site as suggested originally for the  $(\bar{1}11)B$  plane under a GaAs (011) surface [6]. Under larger loads, dislocation loops with Burgers vector normal to the surface ( $b = a/2[0\bar{1}\bar{1}]$ ) reach the back surface. The deviated flow tends to vanish and the 'material transfer' in  $\{111\}$  slip planes normal to the surface becomes more and more pronounced. It is well known that indentation of a semi-infinite half space generates a plastic zone whose radius is 2–3 times the half of the diagonal  $c \sim (2-3) \cdot D/2$  [4, 10, 11]. Under a load of 1.9 N (onset of 'material transfer'), the diagonal is  $D = 67 \mu\text{m}$ , so that the radius of the plastic zone in a semi-infinite sample would range between 67 and 101  $\mu\text{m}$ , respectively. These plastic-zone extensions are of the same magnitude as the thickness of the sample ( $e = 250 \mu\text{m}$ ),  $c/e$  ratio being determined between 0.3 and 0.4. Therefore, it can be concluded that for a  $c/e$  ratio over 30–40% ( $c$  from infinite half-space indentation mechanics), the onset of punching throughout the specimens should be detected.

In conclusion, InP (011) thin foils were indented at elevated temperature (400 °C). Contact behavior is changed drastically when one of the dimensions of the object (here the thickness) is of the same magnitude as the plastic-zone dimension. The changes in plastic flow due to the finite thickness of the samples were studied quantitatively using optical interferometry. We

showed that plastic flow is conservative whether the specimens can or cannot be considered as semi-infinite. Furthermore, the conservation flow equation obtained experimentally (Equation 5) implies that when punching throughout the sample happens, piles ups necessarily vanish and that both events are related.

### Acknowledgment

This work has been supported by the Région Ile de France, by Sesame project 1377 and by the Conseil Régional de l'Essonne.

### References

1. E. LE BOURHIS and G. PATRIARCHE, *Prog. Cryst. Growth Charact. Mater.* **47** (2004) 1.
2. T. SUZUKI and T. OHMURA, *Philos. Mag. A* **74** (1996) 1073.
3. X. J. NING, T. PEREZ and P. PIROUZ, *ibid.* **72** (1995) 837.
4. K. L. JOHNSON, "Contact Mechanics" (Cambridge University Press, 1985).
5. Y. CHOI and S. SURESH, *Scripta Mater.* **48** (2003) 249.
6. L. LARGEAU, G. PATRIARCHE, A. RIVIERE, J. P. RIVIERE and E. LE BOURHIS, *J. Mater. Sci.* **39** (2004) 943.
7. L. LARGEAU, G. PATRIARCHE, E. LE BOURHIS, A. RIVIERE and J. P. RIVIERE, *Philos. Mag. A* **83** (2003) 1653.
8. I. YONENAGA, *J. Phys. France* **7** (1997) 1435.
9. W. C. OLIVER and G. M. PHARR, *J. Mater. Res.* **7** (1992) 1564.
10. L. E. SAMUELS and T. O. MULHEARN, *J. Mech. Phys. Sol.* **5** (1957) 125.
11. M. M. CHAUDHRI, *Acta Mater.* **46** (1998) 3047.

Received 20 April, 2004

and accepted 4 January, 2005